Available online at www.sciencedirect.com

ScienceDirect

Energy Procedia 137 (2017) 89–99

Energy Procedia

www.elsevier.com/locate/procedia

14th Deep Sea Offshore Wind R&D Conference, EERA DeepWind'2017, 18-20 January 2017, Trondheim, Norway

Comparison of numerical response predictions for a bottom-fixed offshore wind turbine

Stian Høegh Sørum[a,*], Jan-Tore H. Horn[a], Jørgen Amdahl[a]

[a]*Centre of Autonomous Marine Operations and Systems (AMOS), Department of Marine Technology, Norwegian University of Science and Technology (NTNU), NO-7491 Trondheim, Norway*

Abstract

Numerical simulations are widely used for response calculations on offshore wind turbines. Code-to-code comparisons are frequently used for verification of the codes, as full-scale measurements can be difficult to obtain. However, most code comparisons performed focus on documenting the responses predicted by the different codes, or on the effect of specific differences between the codes. Little insight is provided to how these differences would affect design calculations, such as the fatigue utilization. In this paper, the response predictions of the programs SIMA, vpOne and FAST are compared using the DTU 10 MW reference wind turbine on a monopile foundation. While differences in the models are first highlighted through a number of simplified load cases, a lifetime fatigue evaluation of the model is then performed for the monopile at mudline. In the deterministic load cases the response of all models are quite similar, while some differences become apparent in the stochastic analysis. For the fatigue calculations, a difference of 14 % is found in the damage equivalent bending moment at mudline. This demonstrates how sensitive the fatigue utilization is to small differences is code capabilities and modelling.

Peer-review under responsibility of SINTEF Energi AS.

Keywords: Bottom-fixed wind turbine; code comparison; stochastic wind and waves; fatigue

1. Introduction

The most widely-used method for analysis of offshore wind turbines (OWTs) is numerical time-domain simulations. However, limited access to full-scale measurements makes it difficult to validate the computer codes against real-life measurements. Software-to-software comparisons have therefore been used extensively in verification of developed codes. Here, the OC3, OC4 and OC5 projects [1–4] stand as the greatest efforts, with a large number of institutions and codes contributing to large-scale comparisons. Other code comparisons have also been performed; either with the introduction of new code features or as more ad-hoc investigations to explain differences between the codes [5–10].

* Corresponding author. Tel.: +47 932 45 097.
E-mail address: stian.h.sorum@ntnu.no

1876-6102
Peer-review under responsibility of SINTEF Energi AS.
10.1016/j.egypro.2017.10.336

In addition to verifying the theory implementations, code-to-code comparisons are suitable for investigating how different solution methods affect the calculation results. A large number of different calculation and solution methods are available and implemented in the different codes. Aerodynamic loads are typically calculated using the blade element momentum theory (BEM), while CFD analyses and generalized dynamic wake are examples of alternative calculation methods[11]. The BEM theory can also include a number of engineering corrections. Wave kinematics can be calculated using linear or higher order wave theory, and integrated to the mean or instantaneous free surface. Furthermore, a number of options are available for modelling of soil-structure interactions. Kühn [12] presents three options for a monopile structure: the use of nonlinear springs along the length of the pile, implementation of a translational and rotational spring at the mudline, or the use of an equivalent cantilever beam. Finally, the structural dynamics can be analysed using either the finite element method, modal analysis, multibody dynamics or a combination of these.

This paper aims at investigating how the calculated fatigue utilization will vary between different computer codes. To do this, the DTU 10 MW reference wind turbine [13] is modelled in SIMA v3.3.2 from SINTEF Ocean, FAST v8 from NREL and vpOne from Virtual Prototyping. The paper will first present the model, before an overview of the theory implementations and modelling capabilities of the codes will be given. Following this, the response to deterministic load cases are presented to easier identify the differences between the codes. Finally, a number of stochastic load cases are analysed before a simplified fatigue analysis is performed.

2. Model Description

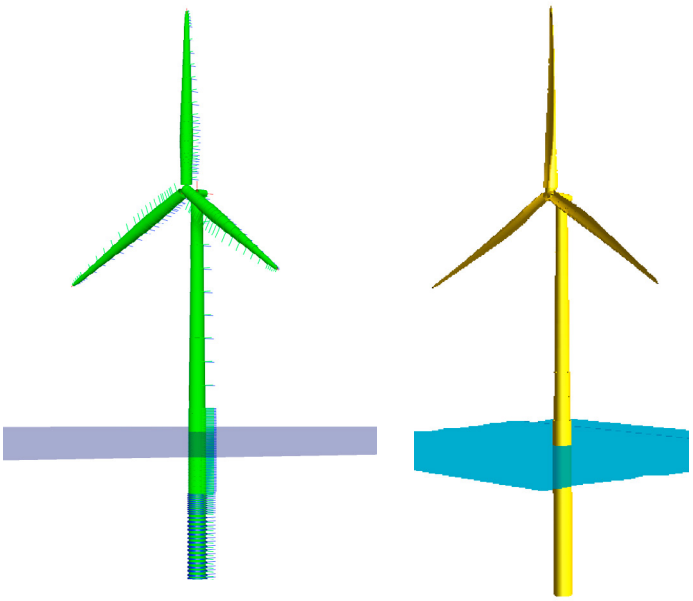

Fig. 1. Model in SIMA (left) and vpOne (right)

The turbine used in the analyses is the DTU 10 MW reference turbine, as described in [13], with the basic DTU 10 MW controller [14]. In order to reduce the natural period, the wall thickness of the tower has been increased by 20 %. Furthermore, the inner foils of the turbine have been modified, both following [15]. The turbine is placed on a monopile foundation in 30 m water depth, which extends to 42 m below the mudline. The transition piece is modelled from 10 m below the mean water level (MWL) to 11.5 m above MWL. Both the transition piece and monopile have an outer diameter of 9 m, while the thickness is set to an equivalent thickness of 0.15 m for the transition piece and 0.11 m for the monopile. Soil properties are taken from Dogger Bank, and the soil is modelled as non-linear springs using the p-y curves in accordance with [16] in SIMA and vpOne. In FAST, an equivalent cantilever beam is used to represent the soil stiffness. Structural damping was modelled as mass and stiffness proportional damping in SIMA

and vpOne, while modal damping was applied in FAST. This was set to be 0.70 % of critical damping at the first and second tower modes. The turbine as modelled in SIMA and vpOne is shown in Figure 1.

3. Program Capabilities

This section briefly presents the capabilities of the three codes, and will furthermore specify which options that have been used in the analyses. For more detailed theory, or description of other capabilities, the reader is referred to the relevant theory manuals [17–22]. A summary of the differences can be found in Table 1, with the exception of the aerodynamics, which is given in Table 2.

Table 1. Differences in code capabilities

	SIMA	VpOne	FAST
Wave Kinematics	Airy or Stokes 5th order (Airy used)	Airy, Stokes 5th order or Stream function (Airy used)	Airy or 2nd order waves (Airy used)
Hydrodynamic stretching	None, Wheeler, constant extrapolation, moving of potential (Wheeler used)	Wheeler or constant extrapolation (Wheeler used)	None
Hydrodynamic load model	Morison, MacCamy & Fuchs (Morison used)	Morison, MacCamy & Fuchs (Morison used)	Morison, potential flow (Morison used)
Soil stiffness model	Non-linear springs	Non-linear springs	Equivalent beam
Structural model	FEM, Beam elements	FEM, Beam elements	Modal model, FEM (modal model used)
Controller type	Java	DLL	DLL

3.1. Aerodynamic Loads

While all three codes utilize BEM theory, there are different corrections implemented in the three codes [17,20], as given in Table 2. Furthermore, the distribution of aerodynamic properties varies between the programs. In SIMA, the aerodynamic properties are specified for each structural element, while FAST defines the properties at given cross sections and interpolates the values. VpOne allows both options to be used, and the SIMA method has been used in the analyses. As an alternative to BEM, FAST can also calculate aerodynamic loads using Generalized Dynamic Wake (GDW), but this is currently not available in the latest version of AeroDyn (v15)[20]. All codes can include tower drag, but this has not been utilized in this paper.

Table 2. Aerodynamic corrections

	SIMA	VpOne	FAST (AeroDyn v15)
Prandtl's correction	Tip loss	Tip loss	Hub & tip loss
Glauert correction	Burton formulation	Two options, as given in [23]	Buhl formulation
Dynamic Wake	Øye model	Øye model	No
Dynamic stall (not used)	Øye model	Øye model	Beddoes-Leishman model
Upwind tower influence	Potential flow	Potential flow	Potential flow
Skewed inflow	Yes	Yes	Yes

3.2. Hydrodynamic Loads

All codes calculate the hydrodynamic loads using Morison's equation, while diffraction can be taken into account using MacCamy & Fuchs correction is SIMA and vpOne [17,18,21]. Furthermore, SIMA and vpOne include the option to extrapolate the wave kinematics to the instantaneous free surface, either by constant extrapolation or Wheeler stretching. As vpOne requires extrapolation of some kind, Wheeler stretching has been used in both the SIMA and vpOne simulations. Stretching is not yet available in FAST v8.

Airy wave theory has been used in all analyses, and the Morison coefficients have been specified to 1.0 and 0.9 for the added mass and drag terms.

3.3. Soil Modelling

SIMA and vpOne both utilize distributed non-linear springs in the soil modelling. In FAST, the soil is modelled using an equivalent cantilever beam. This requires the cantilever to be tuned in order to provide the correct natural period and response, which has been done using the steady state tower top displacement and mudline bending moment as the tuning parameters.

3.4. Structural Model

Both SIMA and vpOne are non-linear finite element analysis programs developed for the offshore industry. While the element formulations differ between the two codes, they both allow for large rotations and displacements, as well as non-linear material behaviour [17,19].

In FAST, the tower and blades are modal models in ElastoDyn, while the equivalent monopile is modelled as a FEM structure and reduced to a modal model using the Craig-Bampton method [22]. The two first tower modes in fore-aft and side-side direction are included together with the two first flapwise modes and first edgewise mode of the blades. It is also possible to model the full structure as finite element models in BeamDyn, but this has not been utilized here.

3.5. RNA Model

How the components in the rotor nacelle assembly (RNA) are modelled also varies between the codes. In both SIMA and FAST, the blade pitch is applied as a prescribed rotation of the blades. This is done differently in vpOne, where the pitch actuators are modelled as torsional springs and a torque is applied to pitch the blades.

Furthermore, both SIMA and vpOne applies the generator torque directly on the shaft, as given by the control system. The drivetrain dynamics are therefore embedded in the shaft properties. In FAST, these dynamics are calculated by a mathematical model of the drivetrain, before the resulting torque is applied to the structural model.

Finally, vpOne and FAST can both use the DTU controller as it is provided. A JAVA version of the controller is required in SIMA, and this may therefore not be as updated as in the other programs. All controllers have been tuned with the same coefficients.

4. Load Cases

In order to compare the predicted response of the turbine, a number of simulations have been run. These are presented in Table 3, where the first three load cases represent deterministic load cases that aim at highlighting the differences among the codes and models. The remaining load cases are stochastic, and aim at illustrating how the code differences influence the predicted response to stochastic loading.

Table 3. Load Cases

Load Case	Simulation type	Wind	Waves	Turbine operational	Tower top
1	Decay test	None	None	No	Free
2	Steady state	Constant uniform	None	Yes	Free
3	Stepped wind	Stepped, uniform	None	Yes	Fixed
4	Turbulent wind	Stochastic, w/shear	None	Yes	Free
5	Irregular waves	None	Irregular	No	Free
6	Combined wind and waves	Stochastic, w/shear	Irregular	Yes	Free

5. Decay Test and Modal Analysis

As a first comparison between the codes, a decay test on a non-operational turbine was performed. The FAST model was subjected to steady, uniform wind speed for 150 s, before the wind speed was abruptly changed to 0.01

m/s. An equivalent force was applied to the tower top of the SIMA and vpOne models, which were released at the same time as the change in wind speed in FAST. Figure 2 shows the decay of the tower base bending moment, and verifies similar damping properties for the models as well as confirming the first natural period of the fore-aft tower motion to be similar. By calculating the logarithmic decrement, the damping level of all models was confirmed.

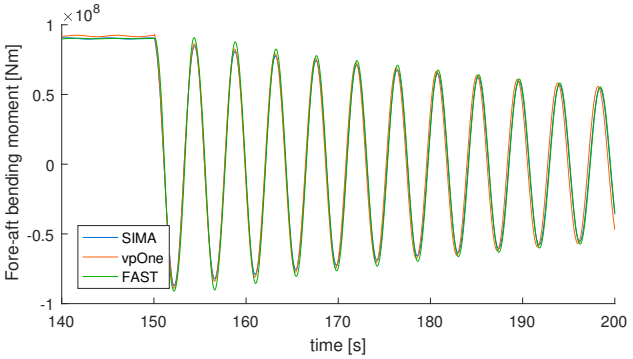

Fig. 2. Decay test

An eigenvalue analysis was also performed in SIMA and vpOne. The natural frequencies of the first modes are given in Table 4 and show reasonable similarities between the models. In FAST, the modes have been identified in the response spectra, and show good agreement with the those obtained with SIMA and vpOne.

Table 4. Eigenfrequencies in [Hz]

	SIMA	vpOne	Difference
1st tower side-to-side	0.227	0.226	0.4 %
1st tower fore-aft	0.228	0.228	0 %
1st blade asymmetric flapwise (yaw)	0.564	0.563	0.2 %
1st blade asymmetric flapwise (pitch)	0.594	0.592	0.3 %
1st blade collective flap	0.624	0.624	0 %
1st blade asymmetric edgewise 1	0.951	0.946	0.5 %
1st blade asymmetric edgewise 2	0.957	0.951	0.6 %
2nd tower side-to-side	1.303	1.241	4.8 %
2nd tower fore-aft	1.189	1.183	0.5 %
2nd blade asymmetric flapwise (yaw)	1.460	1.466	0.5 %
2nd blade asymmetric flapwise (tilt)	1.682	1.715	2 %

6. Wind Only Analysis

6.1. Steady State

To determine the basic aerodynamic and structural properties of the model in each code, the steady state responses were found. The turbines were subjected to constant, uniform wind varying from cut-in to cut-out, and the response after the initial start-up phase was found. For all quantities and wind speeds, the average value over the last 50 s of the analysis was taken as the steady-state solution.

The steady-state solutions are given in Figures 3 and 4. While there in general is good agreement between the three codes, some differences can be noted. For the aerodynamic quantities, FAST returns a lower rotational speed, torque and thereby also power production in the region where the blade pitch is zero. Also, SIMA returns a slightly higher rotational speed than vpOne at 10.5 and 11 m/s, which results in earlier pitching of the blades and a reduction of the thrust force in SIMA. While this can be related to the aerodynamic theories as well as structural and aerodynamic models of the blades, there are also some differences in blade pitch and thereby thrust force at wind speeds above rated.

This may be the result of differences in both the aerodynamics and the way the controller system is implemented in the different codes.

There are also some notable differences in the structural response predicted by the codes. Both the blade tip deflection and tower top displacement show a trend of being larger in vpOne for high wind speeds. This may partially be explained by differences in the predicted thrust, but the tower and foundation also seem to be slightly softer in vpOne. Up to rated wind speed, FAST predicts a lower tower top deflection than the other programs. This can partially be explained by the reduced thrust force in FAST, but also indicates a slightly stiffer structure.

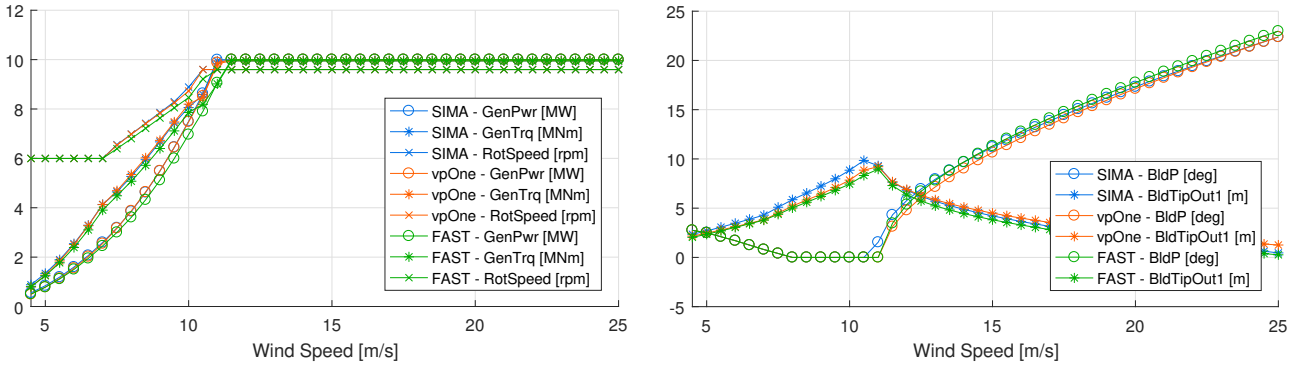

Fig. 3. Steady state responses as function of wind speed. GenPwr = Generator power, GenTrq = Generator torque, RotSpeed = Rotor speed, BldP = Pitch angle of blade 1, BldTipOut1 = Out-of-plane deflection of blade tip, blade 1

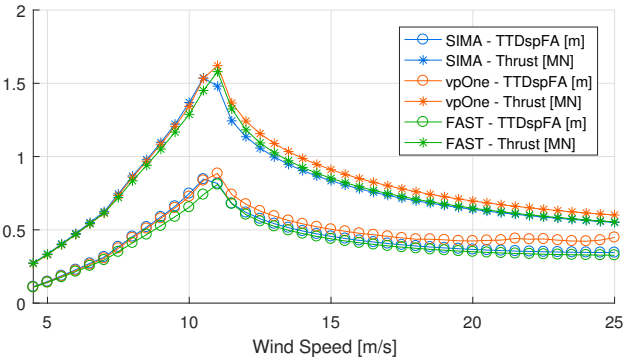

Fig. 4. Steady state responses as function of wind speed. TTDspFA = Fore-aft displacement of tower top, Thrust = Thrust force

6.2. Stepped Wind

The stepped wind analysis was performed to investigate how the control system and aerodynamics work together. With the tower top fixed to eliminate structural motions, the turbine was subjected to steady, uniform wind which was increased in steps of 1 m/s every 50 s, as shown in Figure 5. Some differences between the models become apparent: while FAST converges faster to the steady-state values for wind speeds below rated, SIMA and vpOne converge faster for wind speeds just above rated. For high wind speeds the three models reveal very similar behaviour, with the exception of blade pitch. The blade pitch is however consistent with the steady-state solutions, while the other observed differences indicate that there are some discrepancies in the controller dynamics in the three codes.

6.3. Stochastic Wind

While the above load cases have revealed some difference between the response predicted in the different codes, this does not represent realistic wind loading. The response was therefore analysed in two load cases with turbulent

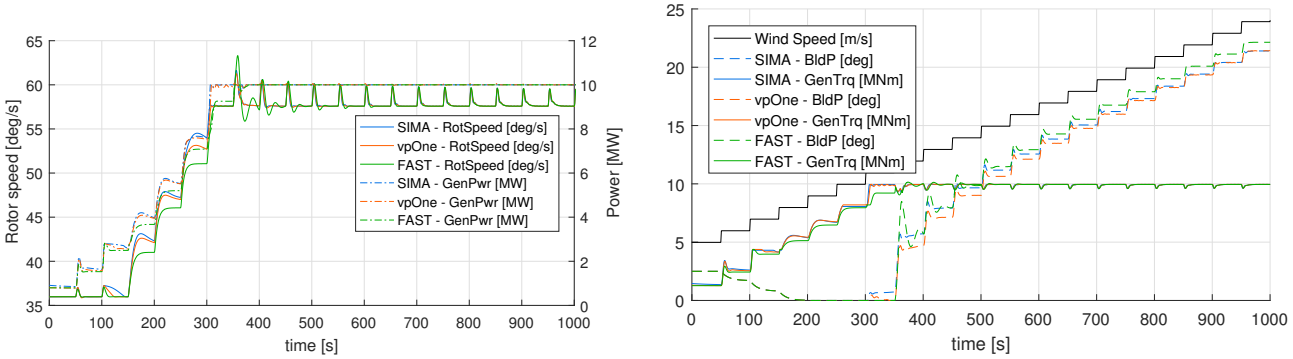

Fig. 5. Response to stepped wind

wind; one with wind speed below rated and one with wind speed above rated. LC 4.1 has a wind speed of 8 m/s measured 100 m above mean sea level, while LC 4.2 has a wind speed of 16 m/s. Both load cases have assumed turbulence class B and a power law exponent of 0.14. Turbsim from NREL has been used to generate 10 minute wind files for each load case, and the calculated spectra are the average of five seeds.

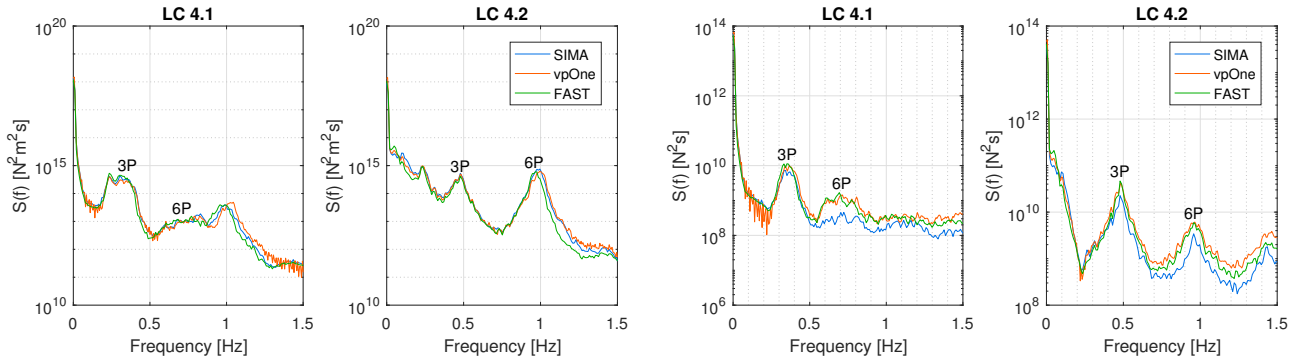

Fig. 6. Response power spectra for mudline moment (left) and thrust force (right) under turbulent wind

Figure 6 shows the response spectra for thrust and mudline bending moment. The spectra for mudline moment shows very similar response characteristics, while SIMA tends to give a lower estimate of thrust force spectrum, especially for the blade passing frequencies.

7. Stochastic Waves

To investigate the hydrodynamic models, two load conditions with irregular waves were analysed; one with a significant wave height of 1 m and peak period of 5 s and one with H_s of 2.5 m and T_p of 7 s. These are denoted respectively LC 5.1 and 5.2. In both conditions, the wave train and resulting wave kinematics are created from a JONSWAP spectrum by the codes. To minimize the aerodynamic damping, the blades were pitched to 82° and the wind speed set to 0.01 m/s.

The response spectra in Figure 7 shows that the base shear reaction is similar in the entire wave frequency range for all three codes, while the response at the first tower bending mode is of different amplitude. The same is seen for the moment at mudline, but this response is completely dominated by resonance.

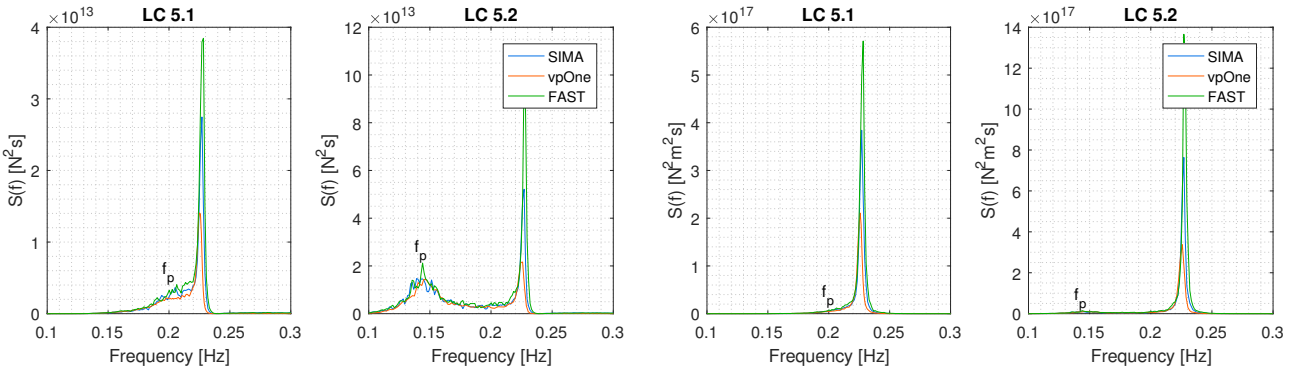

Fig. 7. Response power spectra for base shear (left) and mudline moment (right) under irregular wave loading

8. Combined Wind and Waves

The final analysis was performed for combined wind and wave loading, and were used in both a fatigue analysis and a spectral analysis. First, the results of the fatigue analysis are presented, then a selection of the response spectra are reported for some of the load cases.

The turbine is subjected to turbulent wind, created with TurbSim, and irregular waves generated by the simulation codes. For each condition, five one-hour simulations are carried out in SIMA and FAST, while the results in vpOne are based on 20 ten-minute simulations due to memory limitations in the used version of the program. The environmental data for the simulation parameters are taken from hindcast data provided by the Norwegian Meteorological Institute [24] for the location 54.8 °N, 1.92 °E, which is in the Dogger Bank area. The wind speed is divided into bins of 2 m/s from 4 to 20 m/s, and the most probable sea state for each wind speed is found using bins of 0.5 m for significant wave height and 1 s for the peak period. The resulting environmental conditions are shown in Figure 8, where the condition with the lowest wind speed is denoted LC 6.1 and the condition with the highest wind speed is denoted LC 6.9.

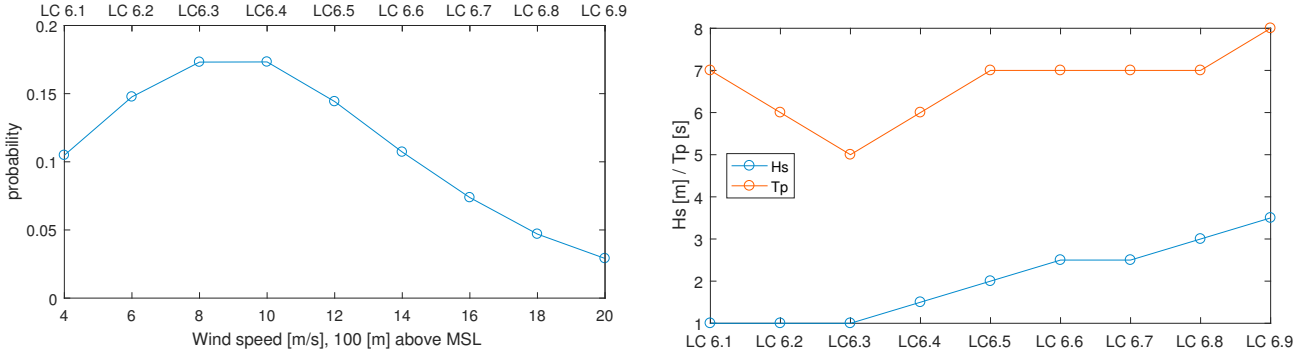

Fig. 8. Wind speed with probability of occurrence (left) and corresponding wave parameters

8.1. Fatigue Analysis

The fatigue utilization at mudline is calculated using the rainflow counting module in the WAFO toolbox for MATLAB [25], S-N curve D for steel in sea water with cathodic protection [26] and an assumed stress concentration factor of 1. For SIMA and FAST, the average utilization during one hour is calculated directly from the simulations, while the 10 minute average utilization from vpOne is scaled up to an equivalent one-hour value. To get the lifetime contribution to fatigue damage over 30 years, each environmental condition is scaled with the probability of occurrence as given in Figure 8.

Some general trends can be observed from the resulting fatigue damage, plotted in Figure 9. FAST does in general calculate higher fatigue damage than the other programs, with the largest difference being at wind speeds in the region

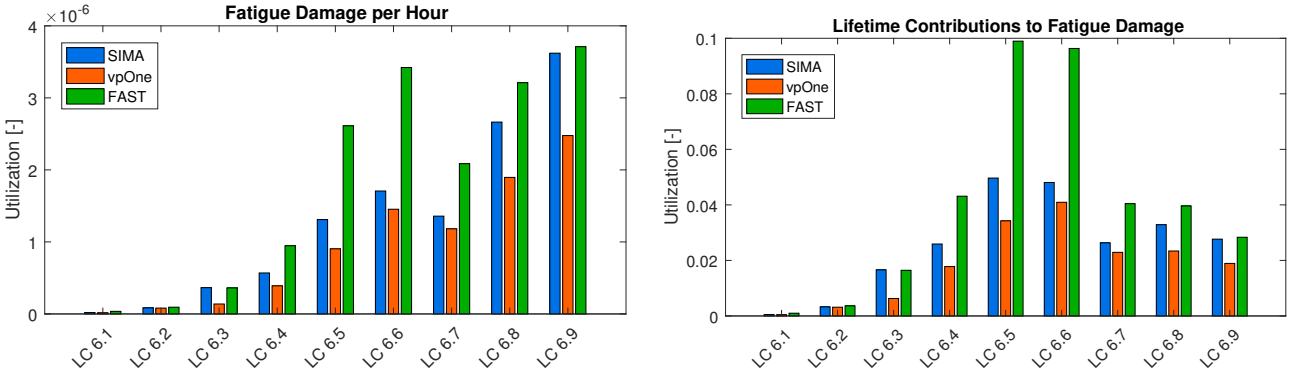

Fig. 9. Utilization in one hour (left) and over 30 years (right)

of 12-14 s, i.e. just above rated wind speed. This is the same region where the controller shows the largest difference in behaviour in the stepped wind analysis, as seen in Figure 5. Another trend is that vpOne returns significantly lower fatigue damage than both FAST and SIMA for high wind speeds and large waves. This indicates that vpOne has a lower response to waves than both SIMA and FAST. A more detailed discussion of this will be given in the next section.

The right plot in Figure 9 shows the fatigue damage contribution for each environmental condition over a lifetime of 30 years. This highlights that the load cases with the highest differences between the predicted results are also those with the largest overall contributions to the fatigue damage. This causes a rather large difference in the predicted total utilization over 30 years, as shown in Table 5. The total damage equivalent load for the mudline bending moment is given in the same table, and shows a 15 % difference between the upper and lower estimates when high-cycle fatigue is assumed.

Table 5. Total fatigue damage

	SIMA	vpOne	FAST
Utilization over 30 years [-]	0.23	0.17	0.37
Damage equivalent load [kNm] (1 [Hz] loading)	1.71	1.60	1.87

8.2. Stochastic Wind and Waves

Using the same simulations as in the fatigue analysis, the power spectra of mudline moment and thrust force are plotted in Figure 10 for LC 6.6 and 6.9 in order to investigate the reason for the differences in fatigue damage in these load cases. For both environments, vpOne seems to have a larger aerodynamic damping of the 1st fore-aft mode of the tower while FAST has the lowest damping. This is consistent with what is seen in the wave-only analysis in Figure 7, and may be explained by the apparently softer tower in vpOne. For both the thrust force and mudline moment, FAST has a peak at approximately 0.05 Hz in LC 6.6. The same peak is less distinct for both SIMA and vpOne, and cannot be identified in LC 6.9. None of the natural frequencies in Table 4 corresponds to 0.05 Hz, but the frequency of the oscillations of blade pitch and rotor speed in Figure 5 is in this frequency range.

9. Discussion

While the models behave similar in the simplified load cases, there is a large difference between the predicted fatigue damage. This is especially caused by differences at wind speeds just above rated, where the fatigue damage can be expected to be dominated by aerodynamic loads. As FAST predicts a larger damage than the other codes, this is likely to be caused by how the aerodynamic properties are defined along the blades.

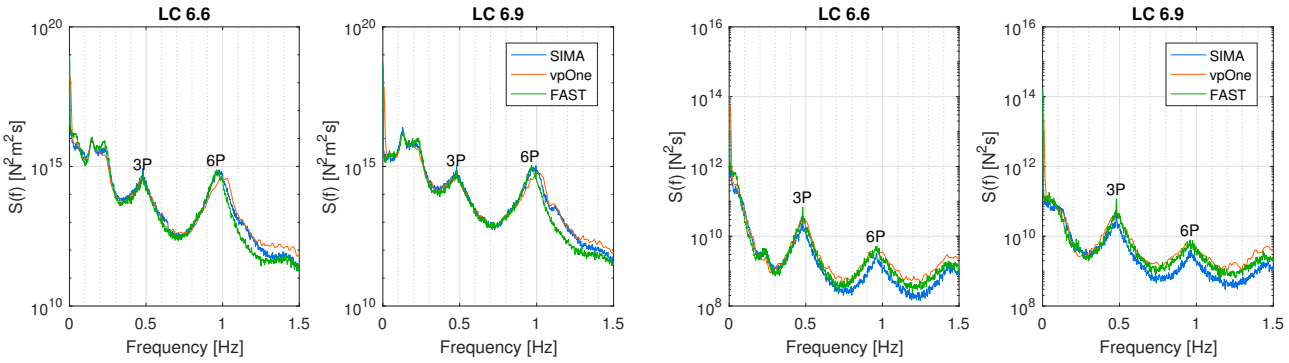

Fig. 10. Response power spectra for mudline moment (left) and thrust force (right) under combined wind and wave loading

Furthermore, the response spectra in FAST shows an increased response at a frequency outside the natural frequencies and load frequencies. This is attributed how the control system and drivetrain interact with the aerodynamic loads. While this could possibly have been achieved by different tuning of the controllers, this shows how the differences between the programs result in discrepancies in the predicted responses if the same system is modelled in each code.

10. Conclusion

The response of the DTU 10 MW reference turbine on a monopile foundation was analysed for a number of deterministic and stochastic load cases using the computer codes SIMA, vpOne and FAST. A number of differences in the predicted responses have been identified. In the final fatigue analysis, the damage equivalent bending moment at mudline was found to vary between 1.60 and 1.87 kNm. The resulting fatigue damage is significantly larger, and the estimated utilization varies between 0.17 and 0.37. This variation is found to be caused by small differences in the predicted tower top displacement, leading to unequal aerodynamic damping, and deviations in the the controller dynamics.

From this, the sensitivity of the calculated response to discrepancies in modelling and code capabilities is highlighted. While the response of the structure to the deterministic load cases are quite similar, the differences result in the large differences in the final fatigue utilization.

Acknowledgements

This work has been carried out at the Centre for Autonomous Marine Operations and Systems (AMOS). The Norwegian Research Council is acknowledged as the main sponsor of NTNU AMOS. This work was supported by the Research Council of Norway through the Centres of Excellence funding scheme, Project number 223254 - AMOS.

References

[1] Jonkman, J., Musial, W.. Offshore code comparison collaboration (OC3) for IEA task 23 offshore wind technology and deployment. Report; NREL; 2010.

[2] Popko, W., Vorpahl, F., Zuga, A., Kohlmeier, M., Jonkman, J., Robertson, A., et al. Offshore code comparison collaboration continuation (OC4), Phase I - results of coupled simulations of an offshore wind turbine with jacket support structure: Preprint. Report; 2012.

[3] Robertson, A., Jonkman, J., Vorpahl, F., Popko, W., Qvist, J., Frøyd, L., et al. Offshore code comparison collaboration continuation within IEA wind task 30: Phase II results regarding a floating semisubmersible wind system. In: ASME 2014 33rd International Conference on Ocean, Offshore and Arctic Engineering; vol. 9B: Ocean Renewable Energy. 2014,.

[4] Robertson, A.N., Wendt, F.F., Jonkman, J.M., Popko, W., Vorpahl, F., Stansberg, C.T., et al. OC5 Project Phase I: Validation of Hydrodynamic Loading on a Fixed Cylinder. Report; NREL; 2015.

[5] Karimirad, M., Meissonnier, Q., Gao, Z., Moan, T.. Hydroelastic code-to-code comparison for a tension leg spar-type floating wind turbine. Marine Structures 2011;24(4):412–435.

[6] Barahona, B., Jonkman, J.M., Damiani, R., Robertson, A., Hayman, G.. Verification of the new FAST v8 Capabilities for the Modeling of Fixed-Bottom Offshore Wind Turbines. AIAA SciTech Forum; American Institute of Aeronautics and Astronautics; 2015,.

[7] Ormberg, H., Bachynski, E.E.. Global analysis of floating wind turbines: Code development, model sensitivity and benchmark study. In: The Twenty-second International Offshore and Polar Engineering Conference. International Society of Offshore and Polar Engineers; 2012,.
[8] Ormberg, H., Passano, E., Luxcey, N.. Global analysis of a floating wind turbine using an aero-hydro-elastic model: Part 1—code development and case study. In: ASME 2011 30th International Conference on Ocean, Offshore and Arctic Engineering. American Society of Mechanical Engineers; 2011, p. 837–847.
[9] Luxcey, N., Ormberg, H., Passano, E.. Global analysis of a floating wind turbine using an aero-hydro-elastic numerical model: Part 2—benchmark study. In: ASME 2011 30th International Conference on Ocean, Offshore and Arctic Engineering. American Society of Mechanical Engineers; 2011, p. 819–827.
[10] Hansen, M.O.L., Aas Jakobsen, K., Holmas, T., Amdahl, J.. VPONE – a new FEM based servo hydro- and aeroelastic code for wind turbines. Proceedings European Offshore Wind 2009 Conference and Exhibition 2009;.
[11] Hansen, M.O.L., Sørensen, J.N., Voutsinas, S., Sørensen, N., Madsen, H.A.. State of the art in wind turbine aerodynamics and aeroelasticity. Progress in Aerospace Sciences 2006;42(4):285–330.
[12] Kühn, M.J.. Dynamics and design optimisation of offshore wind energy conversion systems. Phd thesis; 2001.
[13] Bak, C., Zahle, F., Bitsche, R., Kim, T., Yde, A., Henriksen, L.C., et al. Design and performance of a 10 MW wind turbine. J Wind Energy To be accepted;.
[14] Hansen, M.H., Henriksen, L.C.. Basic DTU wind energy controller. Report; DTU Wind Energy; 2013.
[15] Bachynski, E.E., Ormberg, H.. Hydrodynamic modeling of large-diameter bottom-fixed offshore wind turbines. In: ASME 2015 34th International Conference on Ocean, Offshore and Arctic Engineering. American Society of Mechanical Engineers; 2015,.
[16] The International Organization for Standardization, . ISO 19901-4 Geotechnical and foundation design considerations. 2016.
[17] MARINTEK, . RIFLEX theory manual. Report; MARINTEK; 2015.
[18] USFOS Reality Engineering, . USFOS hydrodynamics. Report; 2010.
[19] SINTEF, . USFOS - a computer program for progressive collapse analysis of steel offshore structures. Theory manual. Report; 1993.
[20] Jonkman, J., Hayman, G.J., J., J.B.. AeroDyn v15 User's Guide and Theory Manual - DRAFT. Report; NREL; 2016.
[21] Jonkman, J., Robertson, A., Hayman, G.J.. HydroDyn User's Guide and Theory Manual. Report; NREL; Undated.
[22] Damiani, J., Jonkman, J., G., H.. SubDynUser's Guide and Theory Manual. Report; NREL; 2015.
[23] Hansen, M.O.L.. Aerodynamics of Wind Turbines. 2nd edition ed.; Earthscan; 2008. ISBN 9781849770408.
[24] Reistad, M., Breivik, O., Haakenstad, H., Aarnes, O.J., Furevik, B.R., Bidlot, J.. A high-resolution hindcast of wind and waves for the North Sea, the Norwegian Sea, and the Barents Sea. Journal of Geophysical Research: Oceans 2011;116(C5).
[25] WAFO-group, . WAFO - A Matlab Toolbox for Analysis of Random Waves and Loads - A Tutorial. Math. Stat., Center for Math. Sci., Lund Univ.; Lund, Sweden; 2011.
[26] DNV GL AS, . DNV-RP-C203 - Fatigue design of offshore steel structures. 2016.